Evaluating Shrinkage Behaviour of Stabilised Cyprus/Kythrea Group Clays Using Close-Range Photogrammetry and Free Shrinkage

A. Ekinci, Y. Bazarbek

European University of Lefke, Lefke, North Cyprus

KEYWORDS: Fibre, Cement, Clay, Shrinkage, Reinforcement, Photogrammetry

ABSTRACT: To mitigate geotechnical problems due to shrinkage of soils, researchers performed studies on mixtures of soil with additives such as lime, cement and/or fibres. Chemical additives tend to generate stiff materials and may leach and create environmental problems; therefore, fibre reinforcement or cement-fibre combinations became an interesting alternative as it reduces the free shrinkage in soils subjected to drying. In this article, results of a pilot study on reinforced and unreinforced slurry samples of clay from the Cyprus Kythrea Group, subjected to desiccation, are presented. The samples were prepared in slurry state by bringing the moisture content of the oven dried clay into 1.5 times the liquid limit. For all monitored specimens, samples were prepared as untreated, 5% cement treated, 1% fibre treated and 5% cement-1% fibre combination by dry weight. While the samples were subjected to air drying, dimensions of the specimens were measured, and photographs were taken. In addition to conventional methods, a complimentary technique, close-range photogrammetry (CRP), is adopted to calculate volumetric shrinkages. The results show that the fibre reinforced, and cement stabilised samples have a lower volumetric deformation and no desiccation cracking was monitored while the unreinforced samples showed a higher volumetric reduction with numerous cracks. Furthermore, the CRP measurements have shown higher accuracy and an alignment with conventional measuring methods.

1 Introduction

With the recent developments of computer processing technology, data storage capacity and digitized image recording and processing systems, Close Range Photogrammetry (CRP) is becoming popular in engineering applications. Development of such technology enabled monitoring of structures remotely at time and access restricted environments. Additionally, such technique is cost effective solution where large amount of geometric information can be acquired in a short period by image acquisition. Furthermore. it allows revisiting the visual records and performing additional analysis at a later time.

Due to such overwhelming benefits, researchers are intensively investigating the further use of Close Range Photogrammetry. This method is used in a wide variety of industries, but it is often ignored in some applications, particularly for deformation monitoring. Luhmann et al. (2013) discuss how CRP can be applied for deformation monitoring, particularly in environments with access and time restrictions. Furthermore, Jiang et al. (2008) highlighted how monitoring of bridges can be carried out routinely using CRP, by aiding findings with evidence of investigations carried out. In another study, Tasci (2013) perform deformation measurements on a steel arch bridge by using CRP. Author compared the CRP analysed deformation behaviour of the steel arch bridge with numerical results generated by using Finite Element Method (FEM). By comparing these methods and processing the data obtained from photographs, the authors confirmed that the CRP results are in agreement with FEM results in terms of detecting displacements. Additionally, Cardenal et al. (2008) successfully used close range photogrammetry for monitoring a landslide in a slope up to 100 m size at Spain. Authors revealed that the CRP measured surface displacement coincides with the inclinometer results available from same site.

Shrink and swell behaviour due to changes in the moisture content is the most important geotechnical problems with clay soils. Such volume changes may cause settlement due to compression, postconsolidation settlement due to shrinkage, heave due to expansion and deformation due to shear stress. Therefore, expansive soils affect the construction and stability of buildings, as described by Najder and Werno (1968), Kumor (1990, 2008), Jez and Jez (2006).

Expansive soil occurs in many parts of the world particularly in arid and semi-arid regions and undergoes significant volumetric changes upon wetting and drying, thus causing ground heave and settlement problems (Chen 1988; Nelson and Miller 1992). Such soils are considered natural hazards and challenge engineers. The estimated damage to buildings, roads, and other structures built on expansive soils, exceeds 10 billion dollars in the US annually (Steinberg 1998; Puppala and Cerato 2009). The total financial loss caused by the expansive soil in a given year surpasses the loss caused due to earthquakes, flood, hurricane and tornadoes (Nelson and Miller 1992).

The mechanism of swelling and shrinking of expansive soils is complex and can be affected by many factors such as the clay content, plasticity, the moisture content and climate (Chen 1988; Nelson and Miller 1992; Houston et al. 2011). Shrinkage and expansion behaviour of the soils is explained by the change in volume resulting from the change in soil water system. The change in soil moisture can disturb the internal stress equilibrium between the clay particles and soil water (Nelson and Miller 1992).

Volume change caused by change in water content resulting in heave or settlement of structures. Chen (1988) has reported many case studies related to the distress caused to the structure due to expansive soil. Clayton et al. (2010) discussed in detailed about the stresses in cast iron pipes due to seasonal shrink and swell of clayey soils. Similarly, Steinberg (1998) explained the various environmental impact of the shrinkage of the expansive soil particularly when it is used as a liner material at the waste disposal site. A variety of research was done in order to eliminate or mitigate the desiccation cracking due to the shrinkage of expansive soils. Albright et al. (2004) have considered the use of surface moisture barriers, placed above the soil layer to be protected. Others have considered soil additives (lime, sand and cement) in order to increase the soil strength and resistance to cracking (Omidi et al. 1996); (Vipulanandan and Leung 1991).

In order to assess the effect of inclusion of fibres into clay, Abdi et al. (2008) and Miller & Rifai (2004) assessed the crack formation and volumetric change over a drying period and wetting/drying cycles. Observations were done using two distinct methods. In the first method, Harianto et al. (2008) monitor the cracks with the naked eye and collect two types of data: volume change (height and diameter measurements) and surface cracking measurements. In the second method, Miller and Rifai (2004) recorded sample geometrical features by using digital imaging software where the crack dimensions are measured using the pixel information of the digital images. The data obtained via this method is used to develop a mathematical model to evaluate the magnitude of the desiccation cracks.

This study mainly aims to develop a methodology to use close range photogrammetry for measurement of free shrinkage potential of highly sensitive Cyprus marl at Laboratory environment to provide cost effective and accurate results. Furthermore, possible shrinkage reduction solutions via cement, fibre and cement-fibre composite addition were investigated.

2 Material Properties

The author recovered block samples during the Spring 2017. The blocks were obtained from the approximately 15m depth of an excevation, located on the Northern Cost of Cyprus, Kyrenia District. The site is located at approximately at Grid Reference 535633E, 3910238N. The site is inclining towards sea with slope angle of approximately 8°. The slope is bound at the top by fields and at the bottom by the sea onto the Mediterranean

The preliminary tests performed were: specific gravity determination, atterberg limit tests and particle size distribution. These tests provide preliminary information for the soil which has been used later, in the analysis. Preliminary tests were also repeated for every other monitored specimens, in order to check the consistency of the used material.

Fig. *1* shows the soil classification curve done in accordance with BS 1377-2:1990. Wet sieving was used to separate the soil into its size frictions. Any soil passing the finest mesh (0.063mm) was subjected to a sedimentation test to determine the distribution down to a particle size of 0.001mm.

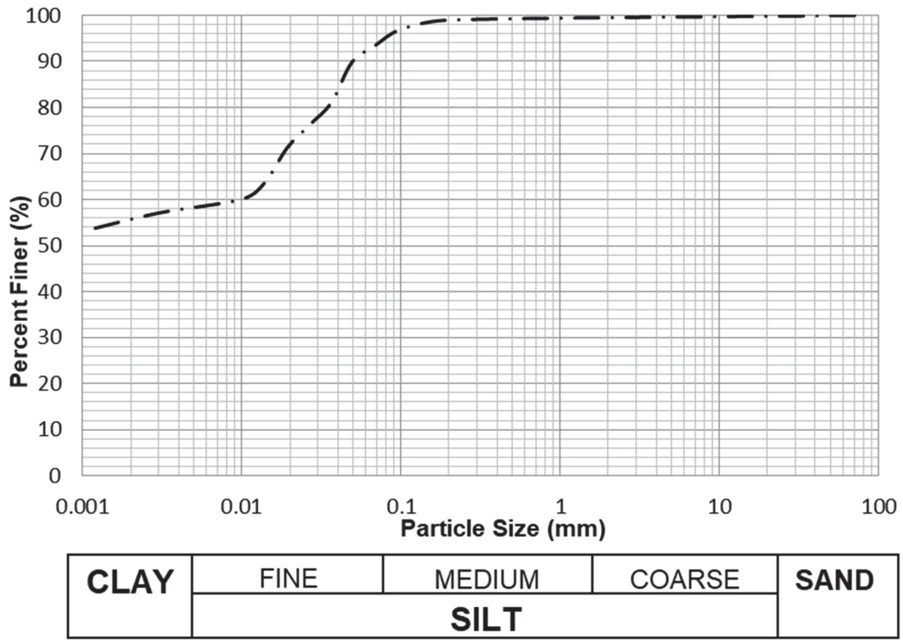

Fig. 1: Particle Size Distribution of Kythrea group Clay

Additionally, Atterberg Limit tests are carried out in accordance to BS 1377-2:1990. The Liquid Limit(W_L), Plastic Limit(P_L) and Plasticity Index(I_p) found to be 47, 22 and 25% respectively. Depending on the results, the above-used clay is classified as inorganic clay of high plasticity (CH), according to USCS classification (ASTM D4318-17e1). Furthermore, the small pyknometer method was used in accordance with BS 1377-2:1990 to determine the specific gravity of clay. The average value of particle density (ρs Avg.) was found to be 2.65 g/ml.

Most of the research on fibre-reinforced soils has made use of polypropylene fibres. It is the most commonly used synthetic material, mainly because of its low cost and environmental acceptability. The polypropylene fibres used in this study have a width of 4mm, length of 63mm and thickness of about 0.021mm. A summary of the properties of the fibres is presented in Table **Tab. 1.**

Tab. 1: Fibre Properties

Properties	Values	Properties	Values
Specific gravity	0.91 g/cm3	Dispersibility	Excellent
Linear mass density	60 Denier*	Melting point	165 °C
Breaking tensile strength	350MPa	Burning point	590 °C
Elastic Modulus	3500MPa	Moisture absorption	0 %

*1Denier=1g/9000m

In this study, Ordinary PC grade 42.5, conforming to ASTM C150M-12, was used in stabilisation purposes. The Blaine fineness and specific gravity of the cement are 289 m^2/ kg and 3.12, respectively

3 METHODOLOGY

3.1 Sample Preparation

In accordance to the above studies samples were prepared in reconstituted state and transferred in split moulds. In total, 30 specimens were prepared in 150 mm diameter and 45 mm height. Specimens were brought to the desired moisture content, around 65%, which is 1.5 wL. Cement was hand-mixed in dry condition at 5% of the dry weight of the soil to achieve a homogeneous distribution where later required water was added and thoroughly mixed and transferred to moulds. Additionally, fibre treated specimens further prepared by addition of 1% of the dry weight of soil as fibre in addition to cement. Following the the casting of specimens, prepared specimens were allowed to set for 2 days before removing from split moulds.

Tab. 2: Treatment properties of tested Specimens

Soil type	No. of Sample	Cement content (%)	Fibre Content (%)
Kythrea	15	0	0
Group	5	5	0
Clay	5	0	1
	5	5	1

3.2 Conventional Measurement Method

Based on the conducted literature review, on the drying techniques, authors believe that there is no single technique that can be claimed to be the best for specimen drying. Therefore, authors decided to use a technique which have been successfully performed in their study of shrinkage behaviour of London clay (Ekinci and Ferreira 2012). In this study, all samples were subjected to air drying, at room temperature, for approximately 30 days. In order to obtain precise measurements, 45 measures (every 10mm interval) were taken from diameter and height of the sample. In order to improve accuracy, all measurements of height and diameter were performed at the same points on each sample. In addition, photographs of specimens have been taken from different angles at same intervals of dimension measurement for the CRP analysis of shrinkage and crack development.

3.3 Close Range Photogrammetry

3.3.1 Testing arrangement

In order to form a reference grid a testing platform have been manufactured as can be seen on Fig. **2**. Base plates of split moulds were kept attached to specimens throughout the monitoring of specimens. Alignment marks were also marked on the base plates in order to locate the specimens at same position on the testing platform at every epoch. Testing platform is a steel plate painted in white in order to make specimens differentiable. Furthermore, artificial targets were installed on the white platform to provide a reference points to align specimens at different epochs. The dimension of the targets are 30 x 30mm and testing platform's size was 1000 x 1000mm.

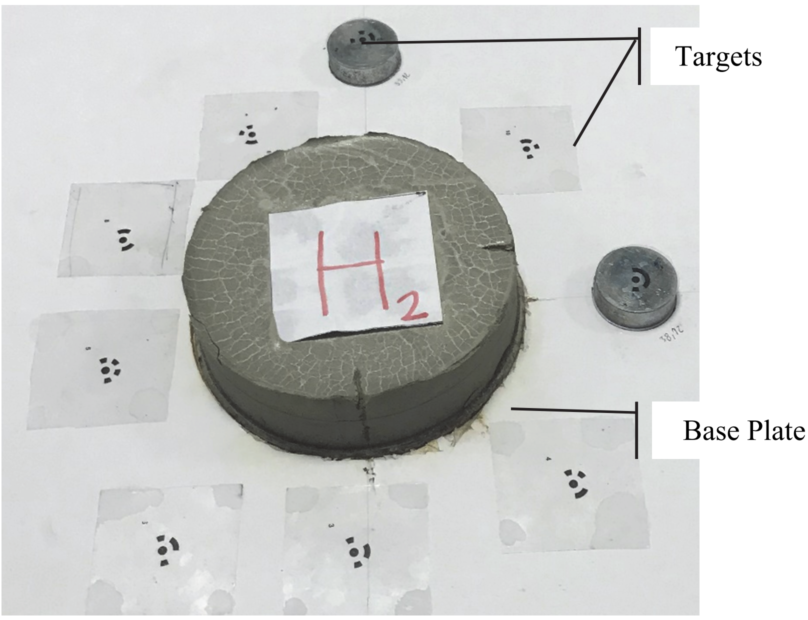

Fig. 2: Photograph of testing platform and referance targets

A widely available smart phone camera was used to take series of overlapping images. Such use of smart phone camera made data acquisition simple. The smart phone was equipped with a wide angle rear camera 12 megapixel, digital zoom up to 5x with a quad-LED "True Tone" flash was used to capture images, this type of lens provides larger area coverage, and fewer images are required to cover the whole platform.

3.3.2 Point Cloud Processing

The commercial software package Agisoft-PhotoScan was used to process the images, to generate the dense point clouds and surface meshes of the tested specimens. For multi-view 3D construction, Photo scan is an affordable solution. Koutsoudis et al., 2013 stated that named software uses Structure from Motion (SFM) and dense multi-view 3D reconstruction algorithms to generate 3D point clouds of an object from a collection of arbitrary taken still images. Furthermore, James and Robson, 2012 reported that the Structure from Motion approach requires multiple pictures of an object or scene from more than one camera positions. Authors also reported that overlapping ratio of at least 70% is required for accurate 3D construction.

Photographs taken at the set intervals were initially downloaded from the camera to the computer. Before loading the photographs into Agisoft- Photo Scan, the captured photos were carefully examined as poor quality and dislocated images can cause disorders in 3D point cloud/model reconstruction. Then raw images in TIFF format were imported into Agisoft- Photo Scan. It is worth to mention that, JPEG, TIFF, PNG, BMP, PPM, Open EXR and JPEG Multi-Picture Format (MPO can also be imported into AgiSoft- Photo scans.

Subsequent to loading photographs to Agisoft-Photo Scan, the first step of the Photogrammetry analysis is to align photographs according to their overlap percentages. The alignment process iteratively refines the external and internal camera orientations and camera locations through a least squares solution. Then software builds a sparse point cloud model (**Fig. *3***). Poor image quality photos should be removed before aligning otherwise can influence the alignment results. Agisoft-Photo scan is capable of analysing image quality based on the sharpness level of the picture.

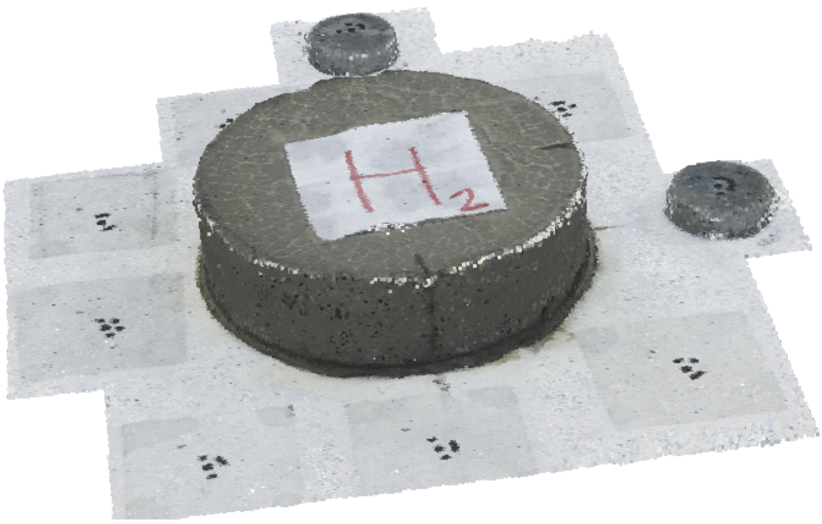

Fig. 3: Agisoft- Photo Scan Point Cloud model of cement treated specimen

Based on the estimated camera positions, the Agisoft-Photo scan software calculates depth information for each camera to be combined into a single dense point cloud. The "Build dense point cloud" command can be selected from the workflow menu. Desired reconstruction parameters can be selected from the build dense cloud dialog box. Quality and depth filtering are the two major parameters that can be set for point cloud generation. Higher quality settings can be used to obtain more detailed and accurate geometry but require a longer time for processing.

3.3.3 Change Detection and Volumetric Analysis

For identifying the shrinkage and cracking behaviour of samples between epochs, generated point cloud data were imported into Cloud Compare software. Cloud Compare is an open source software capable of comparing 3D point clouds in between two epochs or in between point cloud and meshing data. To achieve better comparison between two point clouds, they must be aligned, using Cloud Compare's ICP (Iterative Closed Point processing) algorithm. For a perfect alignment, an overlap between the two point clouds is required. Before performing the alignment and registration of two point clouds, noise and point clouds outside of the area of interest must be removed, otherwise registration could be degraded (Girardeau-Montaut, 2011).

The process of identifying differences of an object by observing it at two epochs is called change detection (Singh, 1989). During the change detection, objects or areas in the point cloud are identified where changes occurred. In a change detection analysis, the unchanged surfaces in a scene are investigated in more detail. The changes that are to be found are in the order of magnitude of the point accuracy, but also in the same order as the noise. The registration of the point clouds influences the accuracy of the point clouds and therefore the possibility to detect changes. An accurate registration is thus an important step.

In order to detect the changes in volume, arrangement shown in **Fig. *4*** called point to surface-based comparison method was performed. There is a function in Cloud Compare that allows the "cloud-to- mesh comparison", where the fitted plane is the mesh. This uses the reference model/mesh as a baseline to compute the volume between the point cloud and the mesh (baseline).

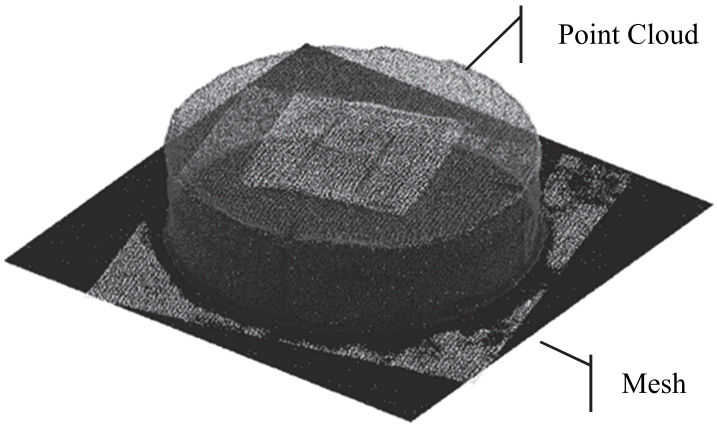

Fig. 4: View from point cloud of cement treated specimen imported from Agisoft-Photo Scan and Mesh created and aligned in Cloud Compare

This function outputs the volume and distance between the point cloud and the mesh as a unitless value. Gaussian distribution of distances from the reference mesh to the cloud displaying a colour coded surface displacement map and a histogram of the specimens. The Gaussian mean was considered as the distance between the mesh and the point cloud for that particular area. **Fig.5** provides an example of the output when comparing the 3D deviation between the baseline and other point clouds, with the scale shown in meters.

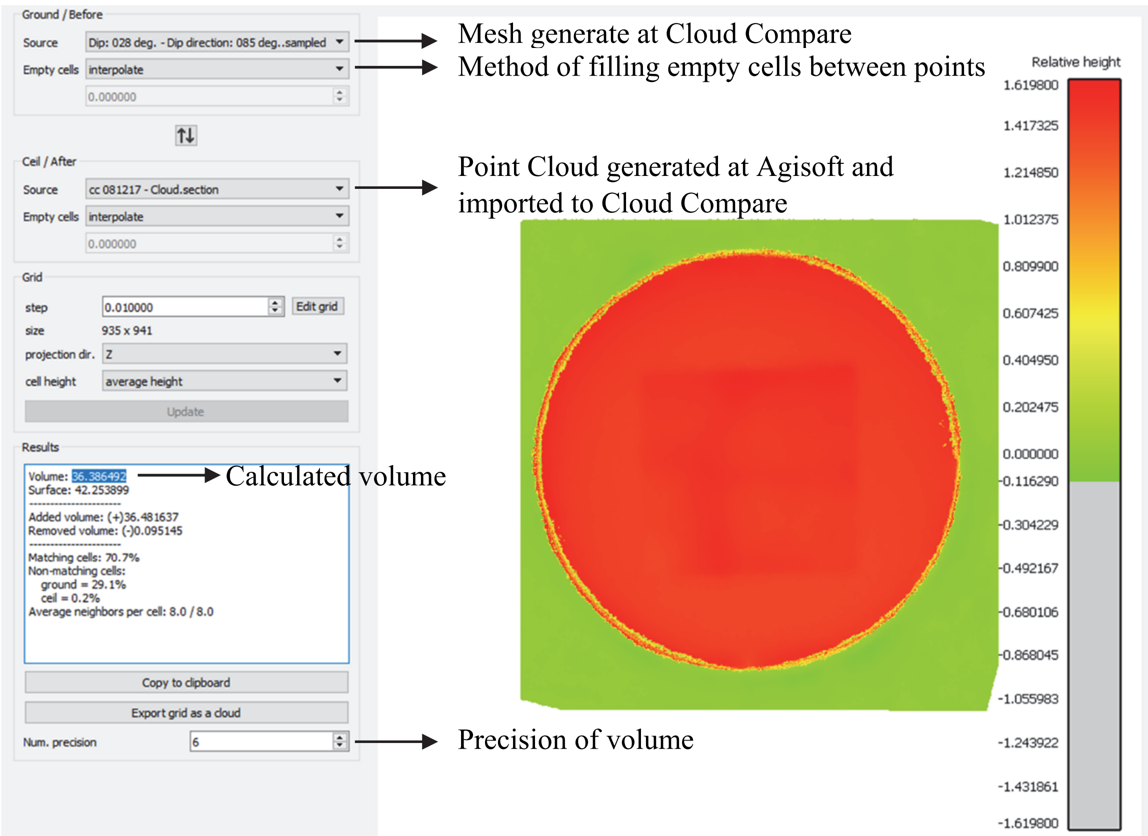

Fig.5: Volume and distance comparison of the cement treated specimen with point to surface-based comparison method.

In this approach created point cloud of two different epoch compared. Regardless of volumetric units measured via cloud compare software, strain reduction of specimens evaluated. Therefore, by knowing the initial volume of the specimens, the desired volume at any epoch can be calculated via interpolation of strain data. Sensitivity of this approach depends on the alignment of specimen in regarding the different epochs. Therefore, grate attention should be taken for the alignment of the targets before the start of the comparison.

4 COMPARISON BETWEEN CONVENTIONAL AND CRP

Data obtained via both Close-Range Photogrammetry and Conventional volume measurement methods of treated and untreated specimens are summarised in Tab. ***3***. Average of Measurements obtained via conventional methods for diameter and height of specimens are used to calculate volume of each specimens. In CRP method the comparison of point cloud of specimen to artificially build mesh enabled to obtain a unitless volume for a specimen at each epoch. The volumes obtained via both methods were normalised by dividing the current volume of specimen V(c) by the initial volume of specimen V(i). As a result the volumetric strain for both conventional and CRP method can be obtained for comparison.

Tab. 3: Data obtained both via Close Range Photogrammetry and Conventional volume measurement methods.

		Cement and Fibre				Cement				Fibre				Clay			
		CRP		Conventional		CRP		Conventional		CRP		Conventional		CRP		Conventional	
Date	Days	Volume (no unit)	Strain	Volume (mm^3)	Strain	Volume (no unit)	Strain	Volume (mm^3)	Strain	Volume (no unit)	Strain	Volume (mm^3)	Strain	Volume (no unit)	Strain	Volume (mm^3)	Strain
08/12/2017	0	15.25	1.00	687756.88	1.00	36.39	1.00	760402.87	1.00	39.85	1.00	636172.51	1.00	59.29	1.00	653843.97	1.00
11/12/2017	3	15.15	0.99	674635.35	0.98	35.28	0.97	734171.07	0.97	36.84	0.92	600234.76	0.94	56.73	0.96	632955.95	0.97
15/12/2017	6	14.02	0.92	639795.43	0.93	33.26	0.91	679253.69	0.89	34.75	0.87	557558.42	0.88	48.85	0.82	519649.71	0.79
18/12/2017	10	13.83	0.91	629551.65	0.92	31.38	0.86	651439.06	0.86	31.18	0.78	518770.43	0.82	45.09	0.76	466089.32	0.71
22/12/2017	13	13.51	0.89	610175.32	0.89	30.17	0.83	619134.54	0.81	29.29	0.74	478525.33	0.75	39.15	0.66	377511.79	0.58
25/12/2017	17	13.08	0.86	597291.67	0.87	28.99	0.80	577494.59	0.76	27.47	0.69	435633.68	0.68	34.34	0.58	365633.68	0.56
28/12/2017	20	12.80	0.84	583589.03	0.85	27.95	0.77	562695.96	0.74	24.45	0.61	402775.24	0.63	32.75	0.55	342775.24	0.52
07/01/2018	30	12.15	0.80	554367.69	0.81	26.89	0.74	554367.69	0.73	23.36	0.59	369438.82	0.58	31.19	0.53	339438.82	0.52

Comparison of Conventional and CRP measured change in normalised Volume of untreated, cement and cement-fibre treated samples free shrinkage behaviour are shown in Fig. ***6***. It can be seen that in untreated samples, immediate reduction in volume have been monitored in 14 days. Furthermore, the fibre and cement only treated samples, experienced smaller volume reductions respectively as compared to untreated specimen. It is clear that the incorporation of the cement-fibre composition enhances the soil resistance to volumetric changes. The results clearly show that the use of cement-fibre treatment of Kythrea Group Clays significantly reduces the volumetric changes.

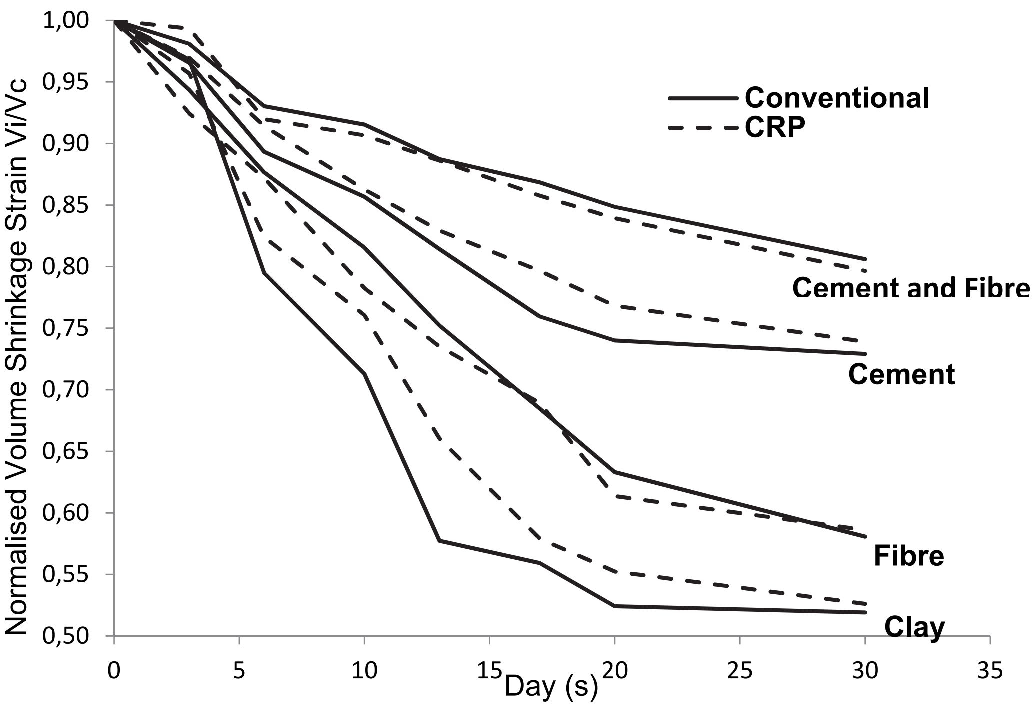

Fig. 6: Comparison of Conventional and CRP measured change in normalised Volume of untreated, cement and cement-fibre treated samples due to drying

It can be seen from both Tab. ***3*** and Fig. ***6*** that the Conventional and CRP measurements are well aligned for all studied samples. Furthermore, it can be seen in Tab. ***4*** that the maximum average difference between the conventional and CRP calculated final volumes of the specimens are less than 3.23%. It can also be observed that with all specimens there is increased differences at certain epochs. This is due to uneven drying pattern and uneven surface due to casting which does not allow the conventional measurements to be done precisely. On the other hand, point to point comparison of the specimen allows more accurate determination of volume calculation which is based on point to point comparison.

Tab. 4: Percentage difference between conventional and CRP methods at each epoch

	Cement and Fibre	**Cement**	**Fibre**	**Clay**
	% Difference			
08/12/2017	0.00	0.00	0.00	0.00
11/12/2017	1.23	0.41	1.91	1.12
15/12/2017	1.05	2.09	0.45	2.91
18/12/2017	0.87	0.58	3.29	4.77
22/12/2017	0.11	1.50	1.71	8.30
25/12/2017	1.08	3.71	0.46	1.99
08/12/2017	0.92	2.82	1.95	2.81
08/12/2017	0.95	1.00	0.54	0.70
Average	**0.89**	**1.73**	**1.47**	**3.23**

5 CONCLUSIONS

The following conclusions are derived based on this study:

- Kythrea group Cyprus clays experienced nearly 50% reduction in volume in 14 days while experiencing free shrinkage.
- Both addition of cement and fibre only in all tested species monitored to reduce the volumetric shrinkage. Nevertheless, Fiber - Cement composition monitored to have ultimate contribution against volumetric reduction.
- It is well proven that the conventional measurement methods require extensive diameter and height measurements to obtain accurate results.
- Maximum average difference between the conventional and Close Range Photogrammetry calculated final volumes of the specimens are less than 3.23%. Furthermore, the study proposed a successful methodology in determination of deformations below 0.1mm
- Fitting an individual mesh to each one of the sample and alignment of targets are important and sensitive tasks which interferes the accuracy of measurements.
- CRP allows further analysis to be done on obtained data at later stages such as crack pattern and quantity studies.
- Success of such study will lead further use of close range photogrammetry in both laboratory and field applications.

6 REFERANCES

Luhmann, T. & Robson, S. (2013) Close-range Photogrammetry and 3D Imaging, De Gruyter.

Jiang, R. & Jáuregui, D.,V. (2008) Close-range photogrammetry applications in bridge measurement: literature review. Measurement 41(8): 823–834.

Cardenal, J, E., Mataa, J, L., Perez-Garcia, J., Delgadoa, M, A., Hernandeza, A., Gonzalezb, J, R. & Diaz-de-Teranb. (2008) Close Range Digital Photogrammetry techniques applied to Landslides monitoring, The International Archives of the Photogrammetry, Remote Sensing and Spatial Information Sciences. Vol. XXXVII. Part B8. Beijing 2008.

Najder, J. & Werno, W. (1968) The effect of climatic fluctuations on displacement of buildings founded on Pliocene clays. Stavebnicky Casopis 2:83–94.

Kumor, M, K. (1990) Awarie budynko´wposadowionych na ekspansywnych iłach trzeciorze˛dowych w Bydgoszczy. Przegla˛d Budowlany 11: 471–476.

Kumor, M, K. (2008) Selected geotechnical problems of expansive clays in the area of Poland. Archit. Civ. Eng. Environ. 1(4):75–92.

Jez, J. & Jez, T. (2006) O awariach budynko´w posadowionych na iłach poznan´skich. Inzynieria i Budownictwo 62(3):135–137.

Puppala, A, J. & A, Cerato. (2009) Heave Distress Problems in Chemically-Treated Sulfate-Laden Materials. Geo-Strata 10 (2): 28–32.

Chen, F., H. (1988) Foundation on Expansive Soils. New York: Elsevier.

Nelson, J, D. & Miller, D, J. (1992) Expansive Soils: Problems and Practice in Foundation and Pavement Design. John Wiley and Sons, New York, NY.

Clayton, C, R., Xu. M., Whiter, J, T., Ham, A,. & Rust, M. (2010) Stresses in cast-iron pipes due to seasonal shrink-swell of clay soils. Proceedings of the Institution of Civil Engineers - Water Management 163(3):157–162.

Steinberg, M. (1998) Geomembranes and the Control of Expansive Soils in Construction. New York: McGraw-Hill.

Omidi, G, H., Thomas, J, C. & Brown, K, W. (1996) Effect of desiccation cracking on the hydraulic conductivity of a compacted clay liner. Water, Air, & Soil Pollution, 89, (1) 91-103.

Vipulanandan, C. & Leung, M. (1991) Seepage Control in Contaminated and Permeable Houston Clay: A Laboratory Study. Hazardous Waste and Hazardous Materials, 8, (1) 17-32.

Abdi, M.R., Parsapajouh, A. & Arjomand, M, A. (2008) Effects of random Finer Inclusion on Consolidation, Hydraulic Conductivity, Swelling, Shrinkage Limit and Desiccation Cracking of Clays. International Journal of Civil Engineering, 6, (4) 23-45

Miller, Carol, J. & Sami, Rifai. (2004) Fiber reinforcement for waste containment soil liners. Journal of Environmental Engineering 130, (8): 891-895.

Harianto, T., Hayashi, S., Du, Y. J., & Suetsugu, D. (2008) Effects of Fiber Additives on the Desiccation Crack Behavior of the Compacted Akaboku Soil as A Material for Landfill Cover Barrier. Water, Air, & Soil Pollution, 194, (1) 141-149.

Ekinci, A. & Ferreira P.M.V (2012) Effects of fibre reinforcement in the shrinkage behaviour of compacted clay. Third International Conference on New Developments in Soil Mechanics and Geotechnical Engineering, 455 - 461.

Koutsoudis, A., Vidmar, B., Ioannakis, G., Arnaoutoglou, F., Pavlidis, G., & Chamzas, C. (2013) Multi-image 3D reconstruction data evaluation. Journal of Cultural Heritage, 15(1), 73–79.

Girardeau-Montaut, D. (2011) Cloud Compare: Cloud to Cloud Compare Workflow. online] Available at: < http://www.danielgm.net/cc/forum/viewtopic.php?f=9&t=105 >

Houston, S. L., Dye, H. B., Zapata, C. E., Walsh, K. D., and Houston, W. N. (2011) Study of Expansive Soils and Residential Foundations on Expansive Soils in Arizona. Journal of Performance of Constructed Facilities, 25(1), 31–44.

Albright, W. H., Benson, C. H., Gee, G. W., Roesler, A. C., Abichou, T., Apiwantragoon, P., Lyles, B. F., and Rock, S. a. (2004) Field water balance of landfill final covers." Journal of environmental quality, 33(6), 2317–2332.

British Standards Institution. (1990) BS 1377-2:1990 Methods of test for soils for civil engineering purposes Part 2: Classification tests." Methods for civil engineering purposes, (1).

ASTM D2487-17. (2018) Standard Practice for Classification of Soils for Engineering Purposes (Unified Soil Classification System), ASTM International, West Conshohocken, PA.

ASTM C150 / C150M-18. (2018) Standard Specification for Portland Cement, ASTM International, West Conshohocken, PA.

Singh, A. (2010) Review Article Digital change detection techniques using remotely-sensed data, International Journal of Remote Sensing, 10:6, 989-1003, DOI: 10.1080/01431168908903939.

Taşçi, L. (2015) Deformation Monitoring in Steel Arch Bridges Through Close□ Range Photogrammetry and the Finite Element Method. Experimental Techniques, 39: 3-10.